

# Testing accuracy of qubit rotations on a public quantum computer

## Supplementary Appendix

Tomasz Białeczki<sup>1</sup>, Tomasz Rybotycki<sup>2,3</sup>, Jakub Tworzydło<sup>1</sup>, and Adam Bednorz<sup>1,\*</sup>

<sup>1</sup>*Faculty of Physics, University of Warsaw, ul. Pasteura 5, PL02-093 Warsaw, Poland*

<sup>2</sup>*Systems Research Institute, Polish Academy of Sciences, 6 Newelska Street, PL01-447 Warsaw, Poland*

<sup>3</sup>*Center for Theoretical Physics, Polish Academy of Sciences, Al. Lotników 32/46, PL02-668 Warsaw, Poland*

Correspondence\*:

Adam Bednorz

Adam.Bednorz@fuw.edu.pl

### SA1 TECHNICAL DETAILS

Each IBM device consists of several connected qubits with available single and two-qubit gates. The sequence of the gates is user-defined. The provided interface allows some fine tuning, like the delay of the gate, using barriers or performing additional resets. Physically the qubits are transmons [1], the artificial quantum states existing due to superconductivity and capacitance (interplay of Josephson effect and capacitive energy). In principle, the transmon has more than two states but the gates' implementation is tailored to limit the working space to two states. The time of decoherence (mostly due to environmental interaction) is sufficiently long to perform a sequence of quantum operations and read out reliable results. The ground state  $|0\rangle$  is the lowest energy eigenstate of the transmon, which can be additionally assured by a reset operation. Gates are time-scheduled microwave pulses prepared by waveform generators and mixers (of length 30 – 70ns with sampling at 0.222ns), taking into account the frequency equivalent to the energy difference between qubit levels [2] (about 4 – 5GHz). The readout is realized by coupling the qubit with a resonator whose frequency depends on the qubit state and measure the phase shift of the populated photons [2, 3].

To run the experiment we had to prepare a script controlling the jobs sent to the computer, lists of individual circuits describing the sequence of the gates and possible parameters, the number of shots, i.e. the number of repetitions of the list of circuits, limited by 8192, later extended to 20000, 32000 and 100000, depending on the device. Each device has some limit on the number of circuits per job. We used lima, jakarta and bogota, as they offered 900 circuits per job running about 100 jobs (later lima and jakarta reduced to 100 and 300, respectively). We also used armonk which is the only single-qubit device, but it offers only 75 circuits per job. In this case, to obtain significant statistics, we had to run more than 1500 jobs. Each circuit consisted of a sequence of gates  $S$  and  $S_\theta$  for  $\theta = j\pi/8$ ,  $j = -7, -6, \dots, 7, 8$  (16 even-spaced values) with additional resets at the beginning and after the readout. This eliminates the effect of daily calibrations. The typical circuit is depicted in Fig. 1 with the actual pulse sequence shown in Fig. 2. To avoid memory effects, we shuffled randomly the values of  $\theta$  individually in each job.

### SA2 RESULTS FROM BOGOTA

The results from the experiment on bogota, Fig. S1 revealed a global phase shift. We are not aware of its reason which can be either due to a wrongly programmed gate or a transpiling error when the script is translated to physical instruction to be performed sequentially on the gates. Nevertheless, the deviations are consistent with other devices if the shift is taken into account. We stress that we used exactly the same script as for the other devices and bogota was neither the first nor the last of the devices to test.

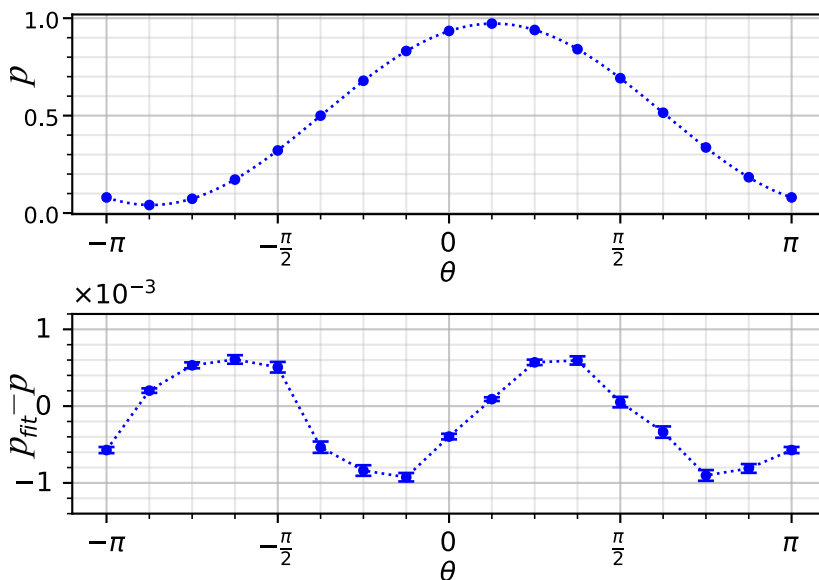


**Figure S1.** The results of the tests  $n = 1$  on bogota, with 100 jobs, 8192 shots per job, and 56 circuits per angle. Notation as in Fig. 3

### SA3 FIRST-ORDER DEVIATIONS FROM IDEAL GATE MODELS

For a general gate (6) we define [4]

$$U_{\theta}(\phi) = \exp \phi (e^{i\theta} |0\rangle \langle 1| + e^{-i\theta} |1\rangle \langle 0|) / 2i = \begin{pmatrix} \cos \phi / 2 & -ie^{i\theta} \sin \phi / 2 \\ -ie^{-i\theta} \sin \phi / 2 & \cos \phi / 2 \end{pmatrix}. \quad (\text{S1})$$

The correction in the first order of  $\epsilon$  to the gate operation (6) reads then

$$\delta(S_{\theta}^n) = S_{\theta}^n \int_0^{n\pi/2} U_{\theta}^{\dagger}(\phi) \begin{pmatrix} 0 & -i\epsilon e^{i\theta} \\ -i\epsilon^* e^{-i\theta} & 0 \end{pmatrix} U_{\theta}(\phi) d\phi / 2 = S_{\theta}^n \int_0^{n\pi/2} H'_{\theta}(\phi) d\phi / 2i, \quad (\text{S2})$$

with

$$H'_{\theta}(\phi) = \begin{pmatrix} \epsilon_i \sin \phi & (\epsilon_r + i\epsilon_i \cos \phi) e^{i\theta} \\ (\epsilon_r - i\epsilon_i \cos \phi) e^{-i\theta} & -\epsilon_i \sin \phi \end{pmatrix}, \quad (\text{S3})$$

assuming  $\epsilon(\theta, \phi + \pi/2) = \epsilon(\theta, \phi)$  (periodicity in  $\phi$  with respect to  $\pi/2$  as the gates are identical). The  $\theta$ -dependent correction to the probability  $p_n(\theta) = |\langle 1| S_{\theta}^n S |0\rangle|^2$  reads

$$\delta p_n(\theta) = -2\text{Re} \langle 0| S^{\dagger} S_{\theta}^{\dagger n} |0\rangle \langle 0| \delta(S_{\theta}^n) S |0\rangle. \quad (\text{S4})$$

Using (4) we calculate

$$\rho = S |0\rangle \langle 0| S^\dagger = \begin{pmatrix} 1 & i \\ -i & 1 \end{pmatrix} / 2. \tag{S5}$$

Denoting

$$\rho_{n\theta} = S_\theta^{\dagger n} M S_\theta^n, \tag{S6}$$

for  $M = |0\rangle \langle 0|$  we get explicitly from (1), (2) and (4)

$$\begin{aligned} \rho_{0\theta} &= \begin{pmatrix} 1 & 0 \\ 0 & 0 \end{pmatrix}, \\ \rho_{1\theta} &= \begin{pmatrix} 1 & -ie^{i\theta} \\ ie^{-i\theta} & 1 \end{pmatrix} / 2, \\ \rho_{2\theta} &= \begin{pmatrix} 0 & 0 \\ 0 & 1 \end{pmatrix}, \\ \rho_{3\theta} &= \begin{pmatrix} 1 & ie^{i\theta} \\ -ie^{-i\theta} & 1 \end{pmatrix} / 2, \end{aligned} \tag{S7}$$

with  $\rho_{n+4,\theta} = \rho_{n,\theta}$ . Substituting (S2), (S5) and (S6) into (S4) we can write the deviation from (3)

$$\delta p_n(\theta) = \int_0^{n\pi/2} d\phi \operatorname{Re} \operatorname{Tr} i \rho_1 \rho_{n\theta} H'_\theta(\phi). \tag{S8}$$

Since  $\rho_1, \rho_{n\theta}, H'_\theta(\phi)$  are Hermitian, we get

$$\delta p_n(\theta) = \int_0^{n\pi/2} d\phi \operatorname{Re} \operatorname{Tr} i \rho_{n\theta} [H'_\theta(\phi), \rho_1] / 2, \tag{S9}$$

with the commutator of  $H'_\theta$  given by Eq.(S3) with  $\rho_1$  given by Eq. (S7)

$$i[H'_\theta(\phi), \rho_1] = \begin{pmatrix} \epsilon_r \cos \theta - \epsilon_i \cos \phi \sin \theta & -\epsilon_i \sin \phi \\ -\epsilon_i \sin \phi & -\epsilon_r \cos \theta + \epsilon_i \cos \phi \sin \theta \end{pmatrix}, \tag{S10}$$

which allows us to derive the final result (7) by plugging  $\rho_n$  given in Eq. (S7) to the trace in Eq.(S9).

## SA4 BENCHMARK

In addition to the main tests, we have checked on lagos how the amplitudes of the fit, i.e. coefficients  $A$  and  $B$  decrease with an increased number  $n$  of  $S_\theta$  gates, in analogy to the standard benchmark tests [5, 6]. The decay of  $A$  and  $B$  over the number of gates corresponds to the decoherence induced by gates and environment. For an odd number  $n$  the signs of  $A$  and  $B$  alternate every two  $S_\theta$  gates. We estimate the error-per-gate  $r$  with a fit to the formula

$$\sqrt{A^2 + B^2} = (1 - r)^n D. \tag{S11}$$

(For even  $n$  the ideal expectation is  $A = B = 0$ , so we don't include these data.)

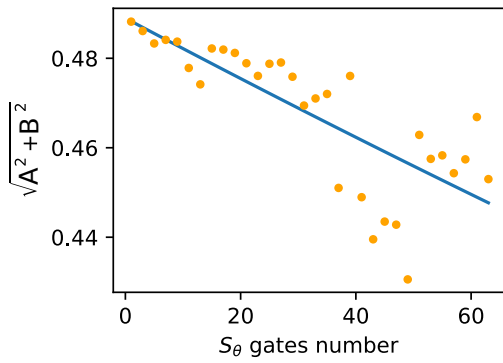


**Figure S2.** The decay of the amplitude  $\sqrt{A^2 + B^2}$  with the number  $n$  of gates ( $n$  is odd). By least squares fit to the formula S11 we estimated  $r \simeq 7 \cdot 10^{-4}$ . The test has been run on lagos with  $n = 63$  jobs, each corresponding to a subsequent number of  $S_\theta$ , 8192 shots per job and 56 circuits per angle.

We found that the error gets accumulated as confirmed by checking the fit after  $n = 62$  and  $n = 63$   $S_\theta$ , see Fig.S3 and cannot be explained by the first order deviations (7) meaning that other effect may be comparable. Nevertheless, the normalized error per gate,  $r \sim 7 \cdot 10^{-4}$ , estimated from the data presented in Fig. S2, remains smaller than our deviations. We conclude that they must have a different origin. In addition, if the error is caused by leakage to other states then it is unlikely that it will cause  $\theta$ -dependent deviation of the same order (at least second order, see Supplementary Appendix SA4).

## SA5 PARAMETER-INDEPENDENT DECOHERENCE

The following reasoning shows that first order correction to the gate channels keeps equal deviations  $\delta p_1 \simeq \delta p_5$ . Introducing standard  $2 \times 2$  Pauli matrices  $\sigma_i$ ,  $i = 1, 2, 3$  and  $\sigma_0$  denoting identity, every qubit state can be written  $\rho = \mathbf{n} \cdot \boldsymbol{\sigma}/2$ , with  $n_1^2 + n_2^2 + n_3^2 \leq 1$ ,  $n_0 = 1$  (equality for pure states). Each quantum channel  $\tilde{R}\rho$  is equivalent to  $R \cdot \mathbf{n}$  with some  $4 \times 4$  matrix  $R$ , whose first row reads  $1, 0, 0, 0$ . In the unitary case,  $R$  contains a rotation matrix in the subspace  $i = 1, 2, 3$ . For the ideal gate  $S_\theta$ , acting in the sense of a quantum channel on density matrices, it is a  $\pi/2$  rotation with eigenvalues  $1, \pm i$ .

The measurement probability reads  $p_k = \text{Tr} M S_\theta^k \rho = \mathbf{m} \cdot S_\theta^k \mathbf{n}$  with  $M = \mathbf{m} \cdot \boldsymbol{\sigma}$ . For a simple, diagonal measurement we specify  $m_1 = m_2 = 0$ , while we keep a general initial state  $\mathbf{n}$ .

We use a polar decomposition of the gate matrix  $S_\theta = U_\theta V D V^{-1} U_\theta^{-1}$ , where

$$U_\theta = \begin{pmatrix} 1 & 0 & 0 & 0 \\ 0 & \cos \theta & -\sin \theta & 0 \\ 0 & \sin \theta & \cos \theta & 0 \\ 0 & 0 & 0 & 1 \end{pmatrix}, \quad V = \begin{pmatrix} 1 & 0 & 0 & 0 \\ 0 & 1 & 0 & 0 \\ 0 & 0 & 1 & 1 \\ 0 & 0 & i & -i \end{pmatrix}, \quad D_\theta = \begin{pmatrix} 1 & 0 & 0 & 0 \\ 0 & 1 & 0 & 0 \\ 0 & 0 & i & 0 \\ 0 & 0 & 0 & -i \end{pmatrix}. \quad (\text{S12})$$

The first order contribution to the difference of deviations from the ideal case comes only from corrections of eigenvalues of  $S_\theta$ , i.e.

$$p_5 - p_1 = 4\mathbf{m} \cdot U_\theta V \delta D_\theta V^{-1} U_\theta^{-1} \mathbf{n}, \quad (\text{S13})$$

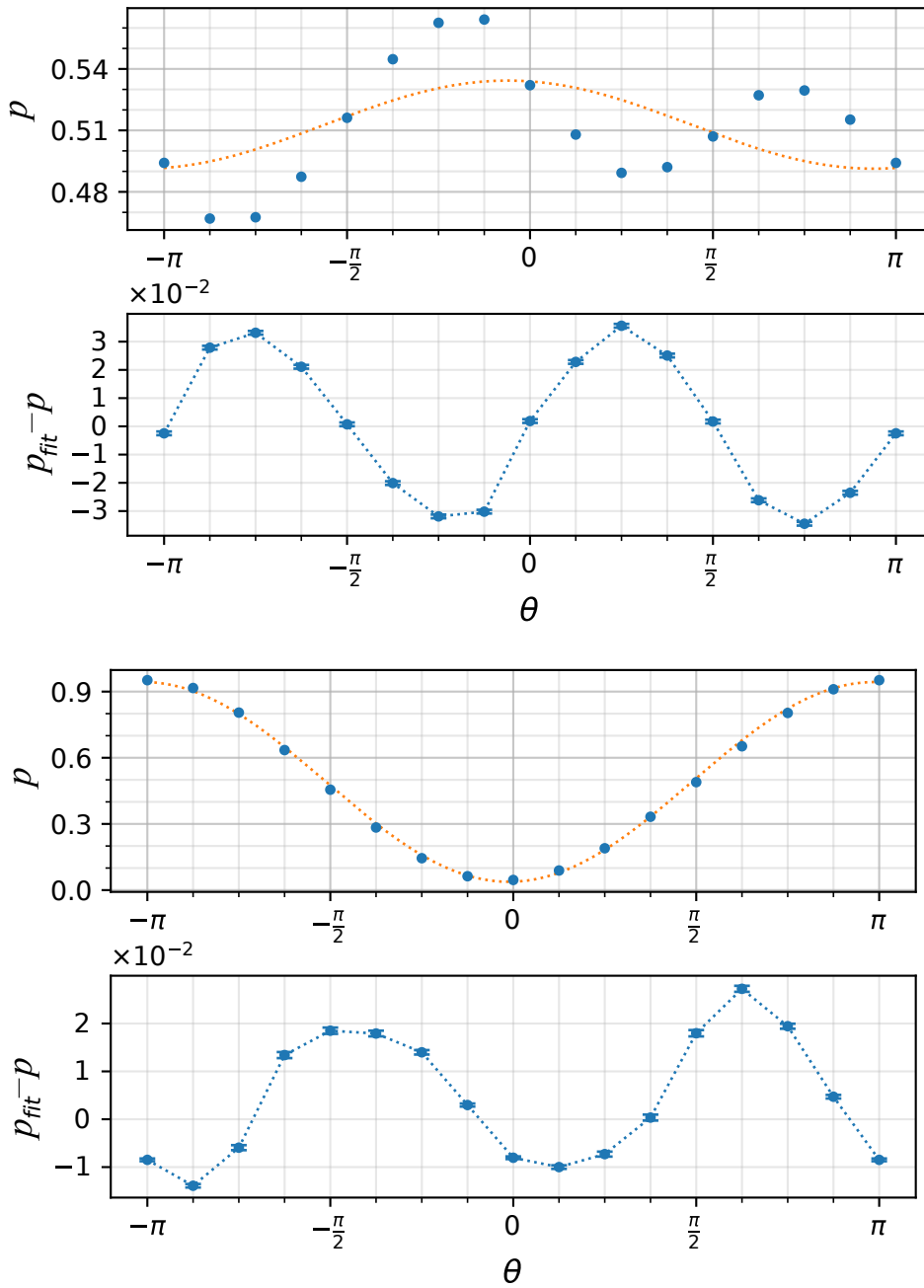


**Figure S3.** The fit to (3) (red dashed line) and deviations (blue dashed line) after  $n = 62$  (upper) and  $n = 63$  (lower)  $S_\theta$ , in the same experiment on lagos as in Fig. S2.

where

$$\delta D_\theta = \begin{pmatrix} 0 & 0 & 0 & 0 \\ 0 & \eta_\theta & 0 & 0 \\ 0 & 0 & \epsilon_\theta & 0 \\ 0 & 0 & 0 & \epsilon_\theta^* \end{pmatrix} \tag{S14}$$

contains empirical parameters  $\eta_\theta \in \mathbb{R}$ ,  $\epsilon_\theta \in \mathbb{C}$ , describing general linear deviations of eigenvalues of  $S_\theta$ .

Assuming preparation of a ground state  $|0\rangle$  initially rotated by  $\pi/2$  around  $x$ -axis, i.e.

$$n_1 = n_3 = 0 \quad (\text{S15})$$

we get  $p_1 - p_5 = 4m_3n_2\text{Im}\epsilon\theta \cos\theta$ . There is no difference between  $p_1$  and  $p_5$  for purely unitary evolution, in linear order in perturbation. As long as  $\xi$  and  $\eta$  remains  $\theta$ -independent,  $p_1 - p_5$  remains a combination of one,  $\cos\theta$ , and  $\sin\theta$  as in (3), even for initial  $\mathbf{n}$  deviating from the ideal case (S15).

Furthermore, a combination of 1, 5, and 9 gates gives

$$p_1 - 2p_5 - p_9 = 4\mathbf{m} \cdot U_\theta V (\delta D_\theta)^2 V^{-1} U_\theta^{-1} \mathbf{n}, \quad (\text{S16})$$

which makes it of the second order in  $\epsilon$ .

A dissipative part can be derived from a generic Lindblad equation

$$\partial_t \rho = i[\rho, H(t)]/\hbar + \sum_m (L_m \rho L_m^\dagger - \{L_m^\dagger L_m, \rho\}/2). \quad (\text{S17})$$

It covers depolarization, phase damping, and relaxation processes [4], which can be described by  $L = \lambda\sigma_3$  or  $L = \lambda\sigma_\pm$  with  $2\sigma_\pm = \sigma_1 \pm i\sigma_2$ . For all such combinations, we can write  $\partial_t \mathbf{n} = H\mathbf{n} + L\mathbf{n}$ , where

$$L = \begin{pmatrix} 0 & 0 & 0 & 0 \\ 0 & A & 0 & 0 \\ 0 & 0 & A & 0 \\ B & 0 & 0 & C \end{pmatrix}, \quad (\text{S18})$$

with some empirical constants  $A, B, C$ , while  $H$  is an infinitesimal rotation. During the gate operation, in the first approximation, we can simply rotate the 1, 2 subspace basis by  $U_\theta$ , same as in (S12),  $H = U_\theta E U_\theta^{-1}$  with some  $\theta$ -independent operation  $E$ . As  $L$  commutes with  $U_\theta$ , the corrections to eigenvalues of  $S_\theta$  will be then also independent of  $\theta$ . As we mentioned earlier, in this case, the difference  $\delta p_1 - \delta p_2$  is incorporated in the fit (3).

## SA6 CORRECTIONS FROM HIGHER STATES

We denote the basis states  $|n\rangle$ ,  $n = 0, 1, 2, \dots$  and set  $\hbar = 1$ . The generic Hamiltonian

$$H = \sum_n \omega_n |n\rangle\langle n| + 2 \cos(\omega t - \theta) \hat{V}(t), \quad (\text{S19})$$

consists of its own energy levels (first term) and the external influence given by frequency  $\omega$ , phase shift  $\theta$ , and the time-dependent pulse  $\hat{V}$  (the second term). In principle free parameters  $\omega, \theta$  and  $\hat{V}(t)$  can model a completely arbitrary evolution. However, the practical realization of gates implies the separation of  $\hat{V}$  into the ideal part and deviations. In this way, we can estimate deviations by perturbative analysis. In addition, we set  $\omega_0 = 0$ ,  $\omega_1 = \omega$  (resonance),  $\omega_2 = 2\omega + \omega'$  (anharmonicity, i.e.  $\omega' \ll \omega$ , here about 300Mhz). We restrict to the states 0, 1, 2 which should contribute to the largest corrections. Rotation and phase can be

incorporated into the definition of states,  $|n\rangle \rightarrow e^{-in(\theta+\omega t)}|n\rangle$ . In the new basis

$$H' = \begin{pmatrix} 2 \cos(\omega t - \theta) V_{00} & (1 + e^{-2i(\theta+\omega t)}) V_{01} & (e^{-i(\theta+\omega t)} + e^{-3i(\theta+\omega t)}) V_{02} \\ (1 + e^{2i(\omega t+\theta)}) V_{10} & 2 \cos(\omega t + \theta) V_{11} & (1 + e^{-2i(\theta+\omega t)}) V_{12} \\ (e^{-i(\theta+\omega t)} + e^{3i(\omega t+\theta)}) V_{20} & (1 + e^{2i(\omega t+\theta)}) V_{21} & 2 \cos(\omega t + \theta) V_{22} + \omega' \end{pmatrix}. \quad (\text{S20})$$

We split  $H' = H_{RWA} + \Delta H$  into the Rotating Wave Approximation (RWA) part

$$H_{RWA} = \begin{pmatrix} 0 & V_{01} & 0 \\ V_{10} & 0 & V_{12} \\ 0 & V_{21} & \omega' \end{pmatrix}, \quad (\text{S21})$$

and correction

$$\Delta H = \begin{pmatrix} 2 \cos(\omega t + \theta) V_{00} & e^{-2i(\theta+\omega t)} V_{01} & (e^{-i(\theta+\omega t)} + e^{-3i(\theta+\omega t)}) V_{02} \\ e^{2i(\omega t+\theta)} V_{10} & 2 \cos(\omega t + \theta) V_{11} & e^{-2i(\theta+\omega t)} V_{12} \\ (e^{-i(\theta+\omega t)} + e^{3i(\omega t+\theta)}) V_{20} & e^{2i(\omega t+\theta)} V_{21} & 2 \cos(\omega t + \theta) V_{22} \end{pmatrix}. \quad (\text{S22})$$

Evolution due to RWA reads

$$U(t) = \mathcal{T} \exp \int_{-\infty}^t H_{RWA}(t') dt' / i. \quad (\text{S23})$$

The full rotation is  $U(+\infty)$ . Only the state  $|2\rangle$  contains the second harmonics  $e^{\pm 2i\theta}$  after restoring original phases.

The 1st order correction to  $U$  reads

$$\Delta U = U(+\infty) \int dt U^\dagger(t) \Delta H(t) U(t) / i. \quad (\text{S24})$$

All terms in  $\Delta H$  with  $\theta$ , contain  $e^{i\omega t}$ , too, which exponentially damps slow-varying expressions, e.g.

$$\int e^{i\omega t} e^{-t^2/2\tau^2} dt \sim e^{-\omega^2\tau^2/2}. \quad (\text{S25})$$

The 2nd order correction reads

$$\Delta^2 U = -U(+\infty) \int dt U^\dagger(t) \Delta H(t) U(t) \int^{t'} dt' U^\dagger(t') \Delta H(t') U(t'). \quad (\text{S26})$$

Most of components get damped exponentially, except when  $\Delta H(t)$  contains  $e^{ik\omega t}$  and  $\Delta H(t')$  contains  $e^{-ik\omega t}$ ,  $k = 1, 2, 3$ , but even then  $k\theta$  gets canceled. Therefore the nonnegligible part of  $\Delta^2 U$  is independent of  $\theta$  (compare with Bloch-Siegert shift [8]), and can be observed as small heating, giving leakage at the level  $10^{-5}$  [9]. Due to a very short sampling time,  $dt = 0.222\text{ns}$ , stroboscopic corrections to RWA [10] can be neglected, too.

## SA7 I/Q IMBALANCE

In reality, the amplitude is a mixture of in-phase and out-of phase (quadrature) components, which may show some imbalance [7] when mixing with local oscillator of frequency  $\omega$ ,

$$V(t) = V_I(t) \cos(\omega t) + V_Q(t)((1 + \varepsilon_1) \sin(\omega t) + \varepsilon_2 \cos(\omega t)), \quad (\text{S27})$$

with

$$V_I(t) = \Omega(t) \cos \theta, \quad V_Q(t) = \Omega(t) \sin \theta. \quad (\text{S28})$$

The minimal model of I/Q imbalance in the basis  $|0\rangle, |1\rangle$  is

$$H = \begin{pmatrix} 0 & \Omega(t)e^{i\omega t}(e^{i\theta} + \varepsilon e^{-i\theta}) \\ \Omega(t)e^{-i\omega t}(e^{-i\theta} + \varepsilon^* e^{i\theta}) & \omega \end{pmatrix}, \quad (\text{S29})$$

where real  $\Omega(t)$  determined the pulse shape and  $\varepsilon = (-\varepsilon_1 - i\varepsilon_2)/2$  is a small constant dimensionless complex number determining I/Q imbalance. With

$$R_t = RR_\omega = \begin{pmatrix} 1 & 0 \\ 0 & e^{i\theta} \end{pmatrix} \begin{pmatrix} 1 & 0 \\ 0 & e^{-i\omega t} \end{pmatrix}, \quad (\text{S30})$$

we remove the rotation of the Hamiltonian

$$R_t^\dagger H R_t - R_t^\dagger \partial_t R_t / i = H' = \begin{pmatrix} 0 & \Omega(t)(1 + \varepsilon e^{-2i\theta}) \\ \Omega(t)(1 + \varepsilon^* e^{2i\theta}) & 0 \end{pmatrix}. \quad (\text{S31})$$

In the following, we exclude the free evolution  $R_\omega$  leaving only  $R$ . Denoting  $\Omega(t) = -d\phi(t)/dt$ , for  $\varepsilon = 0$ , the evolution  $U(t) = \mathcal{T} \exp \int^t H'(t') dt' / i$  is equivalent to (6) with  $\varepsilon = \varepsilon e^{-2i\theta}$  so the correction reads

$$\delta p_{1\theta} = \sin \theta (\sin 2\theta \text{Re} \varepsilon + \cos 2\theta \text{Im} \varepsilon) / 2 \quad (\text{S32})$$

Note the absence of 2nd harmonics so this model is insufficient to explain the found deviations.

## REFERENCES

- [1] Jens Koch, Terri M. Yu, Jay Gambetta, A. A. Houck, D. I. Schuster, J. Majer, Alexandre Blais, M. H. Devoret, S. M. Girvin, R. J. Schoelkopf, Phys. Rev. A 76, 042319 (2007)
- [2] <https://qiskit.org/textbook>
- [3] D. Sank et al., Phys. Rev. Lett. 117, 190503 (2016)
- [4] M. Nielsen, I. Chuang, Quantum Computation and Quantum Information, Cambridge University Press, 2010.
- [5] Max Werninghaus, Daniel J. Egger, Federico Roy, Shai Machnes, Frank K. Wilhelm, Stefan Filipp npj Quantum Information 7, 14 (2021)
- [6] Yuval Baum, Mirko Amico, Sean Howell, Michael Hush, Maggie Liuzzi, Pranav Mundada, Thomas Merkh, Andre R. R. Carvalho, Michael J. Biercuk, arXiv:2105.01079
- [7] David C. McKay, Christopher J. Wood, Sarah Sheldon, Jerry M. Chow, Jay M. Gambetta Phys. Rev. A 96, 022330 (2017)
- [8] F. Bloch and A. Siegert, Phys. Rev. 57, 522 (1940).
- [9] Z. Chen et al., Phys. Rev. Lett. 116, 020501 (2016)

- [10] Daniel Zeuch, Fabian Hassler, Jesse J. Slim, David P. DiVincenzo, *Annals of Physics* 423, 168327 (2020)